

Article

Adsorption of NO₂ and H₂S on ZnGa₂O₄(111) Thin Films: A First-Principles Density Functional Theory Study

Jen-Chuan Tung ¹, Yi-Hung Chiang ², Ding-Yuan Wang ² and Po-Liang Liu ^{2,*}¹ Center for General Education, China Medical University, Taichung 404, Taiwan; jenchuan.tung@gmail.com² Graduate Institute of Precision Engineering, National Chung Hsing University, Taichung 402, Taiwan; ylps51112@gmail.com (Y.-H.C.); ss971331@gmail.com (D.-Y.W.)

* Correspondence: pliu@dragon.nchu.edu.tw; Tel.: +886-921-820915

Received: 4 November 2020; Accepted: 5 December 2020; Published: 9 December 2020

**Featured Application:** This work offers a detailed description of gas-sensing performance of ZnGa₂O₄-based gas sensors.

Abstract: We performed first-principles total-energy density functional calculations to study the reactions of NO₂ and H₂S molecules on Ga–Zn–O-terminated ZnGa₂O₄(111) surfaces. The adsorption reaction and work functions of eight NO₂ and H₂S adsorption models were examined. The bonding of the nitrogen atom from a single NO₂ molecule to the Ga atom of the Ga–Zn–O-terminated ZnGa₂O₄(111) surfaces exhibited a maximum work function change of +0.97 eV. The bond joining the sulfur atom from a single H₂S molecule and the Ga atom of Ga–Zn–O-terminated ZnGa₂O₄(111) surfaces exhibited a maximum work function change of –1.66 eV. Both results concur with previously reported experimental observations for ZnGa₂O₄-based gas sensors.

Keywords: ZnGa₂O₄; NO₂; H₂S; work function; first-principles calculations

1. Introduction

Household and industrial gas sensors are of great significance in artificial intelligence systems [1]. However, several key problems and challenges persist in the development of sensing components. The sensor has an operating temperature that is too high for it to be used as a wearable device; moreover, wearable devices are subject to moisture, which weakens their sensing efficiency. Other problems are the difficulty of distinguishing the composition and concentration of the mixing gases and the inaccuracy of sensing results. Metal oxide compounds, such as tin oxide (SnO₂), gallium oxide (Ga₂O₃), and titanium dioxide (TiO₂) semiconductor materials, have excellent potential for sensing applications and can detect harmful and toxic gases in the temperature range of 300–550 °C [2]. Kolmakov et al., reported that tin oxide nanowire sensors can sense the oxidizing gas of oxygen (O₂) and the reductive gas of carbon monoxide (CO) at temperatures between 200 and 280 °C [3]. Schwebel et al., reported that β-Ga₂O₃ films can be used to sense reductive gases such as CO, hydrogen (H₂), methane (CH₄), nitric oxide (NO), and ammonia (NH₃) [4]. Liu et al., reported that Ga₂O₃ nanowire gas sensors exhibit a reversible response to the oxidizing gases of O₂ and reductive gas of CO in a working temperature range of 100–500 °C [5]. The maximum response of the Ga₂O₃ nanowire gas sensors for CO gas is four times larger than that for hydrogen, ammonia, or hydrogen sulfide (H₂S) gas.

N-type semiconductors of ZnGa₂O₄ thin films have been developed, and ZnGa₂O₄ materials have been successfully used as gas sensors. Satyanarayana et al., reported that spinel ZnGa₂O₄ films can be used to sense liquid petroleum gas (LPG) at temperatures ranging from 200 to 400 °C. ZnGa₂O₄ sensors

doped with palladium at approximately 320 °C have high selectivity to LPG, but poor sensitivity to CH₄ and CO [6]. Furthermore, Jiao et al., reported the use of ZnGa₂O₄ prepared by spraying coprecipitation for sensing LPG, CO, ethanol (C₂H₅OH), and methane [7]. A novel approach described in Chen et al., (2010) [8] is based on the use of ZnGa₂O₄/ZnO core-shell nanowires. Sensitivity to nitrogen dioxide (NO₂) gas can be considerably improved by using ZnGa₂O₄/ZnO core-shell nanowires rather than pure ZnO nanowires. Despite the introduction of new approaches to developing gas sensors, the fundamental interaction between gas molecules and metal oxide compounds remains unclear.

Density functional theory (DFT) calculations have been widely used in the fields of atomic and molecular adsorption on surfaces and the gas-sensing mechanism [9,10]. For example, water adsorption on the carbon nanotube field-effect transistor (CNTFET) explains the humidity-induced hysteresis, and it can be reasoned that water adsorption on the CNTFET leads to an increased chemical activity, the modification of the Schottky barrier, and the adsorption of some ionic substances in the vicinity of the carbon nanotube [9]. The gas-sensing mechanism of ZnO applied to H₂, NH₃, CO, and C₂H₅OH was established by conducting first-principles DFT calculations [10]. When the gas molecules, i.e., H₂, NH₃, CO, and C₂H₅OH molecules, become incident upon the ZnO(10-10) surface, the adsorption-induced reconstruction of the ZnO surface and charge transfer from the gas molecules to the ZnO surface control the sensing process evaluated by the change of electronic conductance of ZnO. Vorobyeva et al., reported that the resistance response of ZnO at operating temperature 450 °C increased (decreased) in the presence of NO₂ (H₂S) [11]. Moreover, the sensor responses of ZnO and ZnO with gallium contents of 0.5% and 4.0 at% show that an increase of gallium caused a monotonous decrease of the sensor response to H₂S due to the enhanced electron-donor ability of surface oxygen anions, the H-S bond-breaking in the H₂S molecule, as well as the decrease of the H₂S adsorption. Recently, we demonstrated epitaxial growth of ZnGa₂O₄ thin film grown on the sapphire substrate using a metalorganic chemical vapor deposition (MOCVD) technique that yields a high-selectivity gas sensor [12]. The ZnGa₂O₄ gas sensor has superior selectivity to NO at the operating temperature of 300 °C. Reactions of NO molecules on Ga-Zn-O-terminated ZnGa₂O₄(111) surfaces were modeled and carried out using a first-principles density functional theory method. The NO molecules combine with the gallium atoms on the ZnGa₂O₄(111) surface to produce N-Ga bonds, leading to the work function changes. The sensor response can be gained from the changes in the work functions, indicating that the N-Ga bonding exhibits a very sensitive adsorption response. In this study, we developed adequate models for accurately predicting toxic NO₂ oxidizing gases and H₂S reducing gases adsorbed on the ZnGa₂O₄(111) surface, which offer a detailed description of gas-sensing performance of the use of ZnGa₂O₄-based thin-film sensors, which may be probed experimentally using phenomenological techniques of sensor characterization such as chemical components, sensing layers, and surface modification by metal doping.

2. Computational Details

A series of ab initio calculations were performed to evaluate the adsorption reactions and work functions of NO₂ and H₂S on ZnGa₂O₄(111) surfaces. The ab initio theoretical results were implemented in the Vienna ab initio simulation package [13,14], and the exchange correlation function was predicted using the generalized gradient approximation (GGA) with the Perdew-Wang (PW91) correction [15,16]. The crystal structure of ZnGa₂O₄ is displayed in Figure 1. The space group for ZnGa₂O₄ is *Fd-3m*, which contains 56 atoms, comprising 8 Zn, 16 Ga, and 32 O atoms. The cutoff energy was set as 400 eV. To simulate the change of the work function with and without an NO₂ or H₂S molecule, we developed a supercell of ZnGa₂O₄ along the (111) direction. This supercell contained 112 atoms, and the vacuum was set to 20 Å. The stoichiometry of all supercells was fixed at Zn₁₆Ga₃₂O₆₄. We used the preferred Ga-Zn-O-terminated surface of ZnGa₂O₄(111) with a surface energy of 0.10 eV/Å² [17]. A gamma-centered 3 × 3 × 1 Monkhorst-Pack grid was used. This supercell was fully relaxed until the force acting on each atom was less than 0.001 eV/Å.

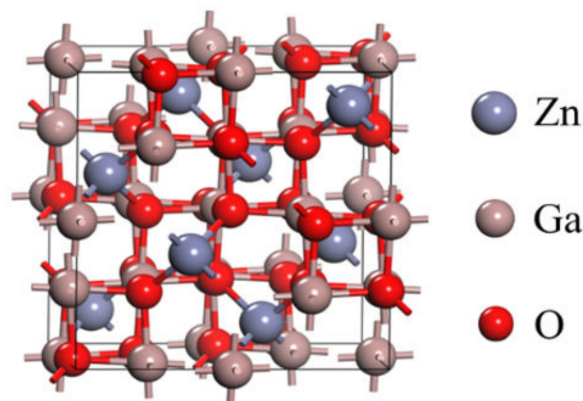


Figure 1. Atomistic representation of bulk ZnGa_2O_4 . Atoms are represented by spheres: Zn (purple, large), Ga (brown, medium-sized), and O (red, small).

To determine the most favorable adsorption site of NO_2 (H_2S) molecules on the $\text{ZnGa}_2\text{O}_4(111)$ surface, we labeled the surface atoms as Ga_{3c} , Zn_{3c} , O_{3c} , and O_{4c} in the top and side views of Figure 2.

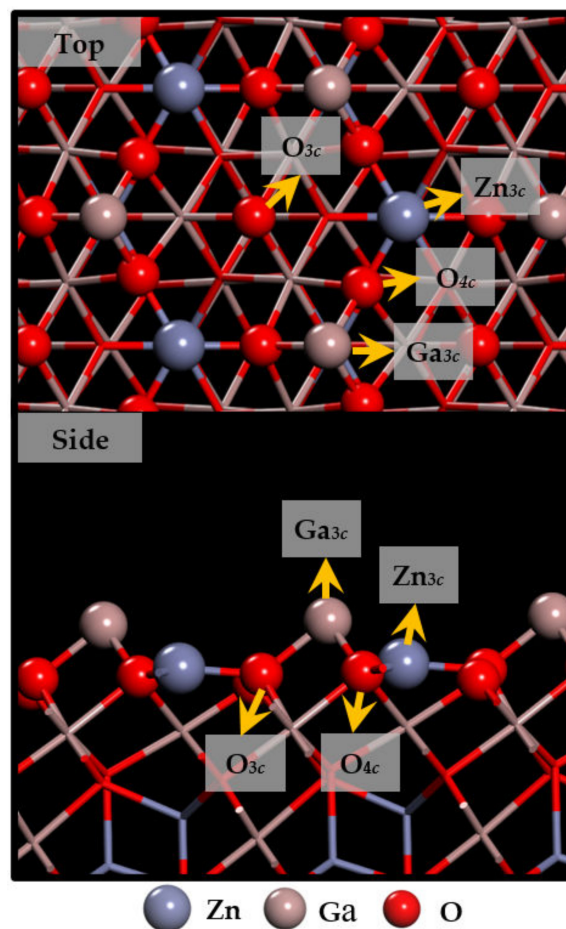


Figure 2. Top and side views of the $\text{ZnGa}_2\text{O}_4(111)$ surface. Surface atoms are labeled Ga_{3c} , Zn_{3c} , O_{3c} , and O_{4c} . Atoms are represented by spheres: Zn (purple, large), Ga (brown, medium-sized), and O (red, small).

We first calculated the work function using the formula [18]

$$\Phi_{\text{ZGO}} = E_{\text{VAC}} - E_{\text{F}} \quad (1)$$

where Φ_{ZGO} is the work function for the clean $ZnGa_2O_4(111)$ surface and E_{VAC} and E_F are the energy of the vacuum and the Fermi energy, respectively. Similarly, when the NO_2 (H_2S) molecule was adsorbed on the $ZnGa_2O_4(111)$ surface, we also calculated the work function Φ_{NO_2} and Φ_{H_2S} , which in turn determined the work function differences $\Delta\Phi$ (eV) between Φ_{ZGO} and Φ_{NO_2} (Φ_{H_2S}). The binding energy E_B (eV/u. c.) is also an important factor determining gas-sensing performance and can be defined as

$$E_B = E_{total} - E_{ZGO} - E_{NO_2/H_2S} \quad (2)$$

where E_{total} is the total energy of the NO_2 (H_2S) molecule adsorbed on the $ZnGa_2O_4(111)$ surface, and E_{ZGO} and E_{NO_2/H_2S} are the total energies of the slab of $ZnGa_2O_4(111)$ surface and the free or isolated NO_2 (H_2S) molecule, respectively.

First, we constructed eight adsorption models, denoted N1, N2, N3, N4, O1, O2, O3, and O4. Here, N (O) represents a nitrogen (oxygen) atom in NO_2 , and numbers "1", "2", "3", and "4" respectively indicate the initial adsorbed Ga_{3c} , Zn_{3c} , O_{3c} , and O_{4c} atom on the $ZnGa_2O_4(111)$ surface. The initial distance of the NO_2 molecule to the $ZnGa_2O_4(111)$ surface was set as the sum of the van der Waal radii of N (O) for the NO_2 molecule and Ga (Zn or O) for surface atoms. Similarly, for the H_2S molecule adsorbed on the $ZnGa_2O_4(111)$ surface, we also developed eight adsorption models, denoted S1, S2, S3, S4, H1, H2, H3, and H4. Here, S (H) represents a sulfur (hydrogen) atom in H_2S . The initial distance of the H_2S molecule to the $ZnGa_2O_4(111)$ surface was also set as the sum of the van der Waal radii of H (S) and Ga (Zn or O) for surface atoms. We performed structure optimization in each model until the force acting on each atom was less than 0.001 eV/\AA , yielding optimized atomic structures.

The gas sensitivity could be determined from the ratio of the resistance in the presence of the investigated gas (R_g) to the resistance in the reference gas (R_a), which is usually air [19]. The relation of gas sensitivity to the work function difference $\Delta\Phi$ is represented by the following equation:

$$\Delta\Phi = \Delta X + kT \ln(R_g/R_a) \quad (3)$$

where ΔX denotes the change in electron affinity and kT denotes the product of the Boltzmann constant k and the temperature T . The upward bending of the surface band due to the adsorption of oxidizing gas on $ZnGa_2O_4(111)$ results in the depletion of free charge carriers on the surface, thus leading to the formation of a region with high ohmic resistance or a positive work function difference. However, the resistance of $ZnGa_2O_4(111)$ gas sensors decreases under exposure to reducing gases because of the downward bending of the surface band, resulting in a negative work function difference.

3. Results and Discussion

The most favorable configurations for NO_2 on $ZnGa_2O_4(111)$ surfaces are shown in Figure 3. In Model N1, the nitrogen atom of the NO_2 molecule was adsorbed on the Ga_{3c} atom of the $ZnGa_2O_4(111)$ surface to yield a N–Ga bond with a bond length of 2.01 \AA . In Model N2, the NO_2 molecule moved away from the originally adsorbed Zn_{3c} atom to approach the neighboring Ga atom of the $ZnGa_2O_4(111)$ surface to form an O–Ga bond with a bond length of 1.90 \AA . In Model N3, the NO_2 molecule moved away from the originally adsorbed O_{3c} atom toward the neighboring Ga and Zn atoms of the $ZnGa_2O_4(111)$ surface to form N–Ga and O–Zn bonds with bond lengths of 2.05 \AA and 2.30 \AA , respectively. In Model N4, the nitrogen (oxygen) atom of the NO_2 molecule adsorbed on the Ga_{3c} (Zn_{3c}) atom of the $ZnGa_2O_4(111)$ surface to form an N–Ga (O–Zn) bond with a bond length of 2.06 \AA (2.21 \AA). In Model O1, the two O atoms of the NO_2 molecule adsorbed on the Ga_{3c} atom of the $ZnGa_2O_4(111)$ surface to yield two O–Ga bonds with bond lengths of 2.07 \AA and 2.13 \AA . Similarly, in Model O2 (O3), the NO_2 molecule moved away from the originally adsorbed Zn_{3c} (O_{3c}) atom toward the neighboring Ga_{3c} atom of the $ZnGa_2O_4(111)$ surface to form two O–Ga bonds with bond lengths of 2.10 (2.13) \AA and 2.11 (2.08) \AA . In Model O4, an O atom of the NO_2 molecule was adsorbed on the Ga_{3c} atom of the $ZnGa_2O_4(111)$ surface to form an O–Ga bond with a bond length of 1.92 \AA . The vacuum energy, Fermi energy, work functions of $ZnGa_2O_4(111)$ with and without NO_2 , and work function difference among

NO_2 adsorption models are presented in Table 1. The work function increased when the NO_2 molecule was adsorbed on the $\text{ZnGa}_2\text{O}_4(111)$ surface. The increase in work function ranged from +0.29 eV to +0.97 eV, which concurs with previously reported experimental results of similar resistance responses of $\text{ZnO}(\text{Ga})$ samples to NO_2 [8,11]. The NO_2 molecule preferred bonding with the Ga_{3c} or Zn_{3c} atom. Model N1 had the maximum work function difference of +0.97 eV, exhibiting increased sensitivity for detecting NO_2 molecules.

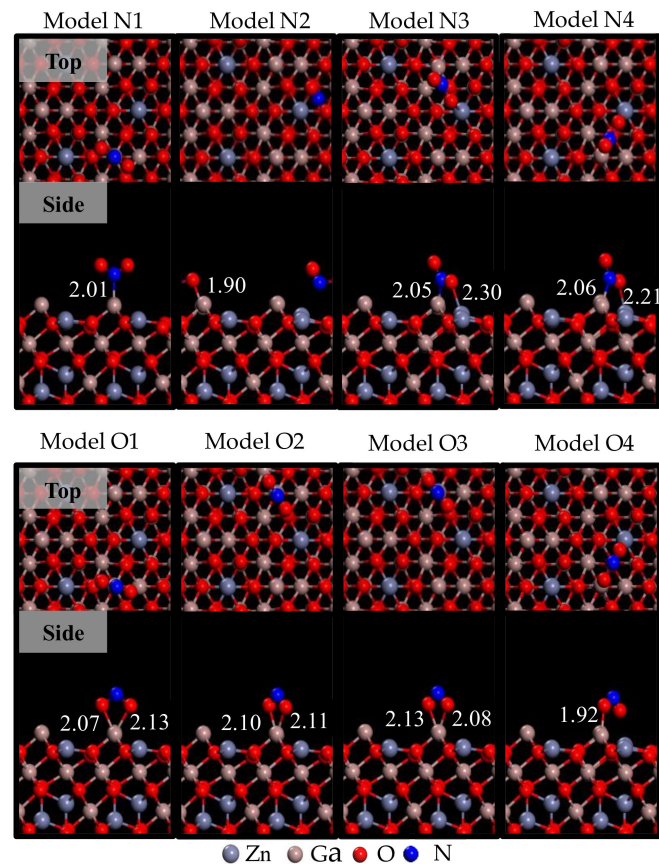


Figure 3. Top and side views of the favorable configurations for NO_2 on the $\text{ZnGa}_2\text{O}_4(111)$ surface. Atoms are represented by spheres: Zn (purple, large), Ga (brown, large), S (yellow, medium-sized), O (red, medium-sized), and H (white, small). Equilibrium bond lengths between molecular and surface atoms are given in Angstrom.

Table 1. Calculated vacuum energy E_{VAC} , Fermi energy E_F , work function of NO_2 Φ_{NO_2} , work function of $\text{ZnGa}_2\text{O}_4(111)$ Φ_{ZGO} , and work function difference $\Delta\Phi$ ($\Delta\Phi = \Phi_{\text{NO}_2} - \Phi_{\text{ZGO}}$) among the eight NO_2 adsorption models. All energies are presented in eV.

Models	Adsorption Sites	E_{VAC}	E_F	Φ_{NO_2}	Φ_{ZGO}	$\Delta\Phi$
$\text{ZnGa}_2\text{O}_4(111)$	-	0.66	-3.38	-	4.04	-
N1	Ga_{3c}	1.45	-3.56	5.01	-	+0.97
N2	Ga_{3c}	1.04	-3.29	4.33	-	+0.29
N3	$\text{Ga}_{3c}, \text{Zn}_{3c}$	1.12	-3.31	4.43	-	+0.39
N4	$\text{Ga}_{3c}, \text{Zn}_{3c}$	1.09	-3.31	4.40	-	+0.36
O1	Ga_{3c}	0.98	-3.41	4.39	-	+0.35
O2	Ga_{3c}	1.01	-3.36	4.37	-	+0.33
O3	Ga_{3c}	1.07	-3.31	4.38	-	+0.34
O4	Ga_{3c}	1.04	-3.29	4.33	-	+0.29

Figure 4 displays the lowest energy configurations for H₂S on ZnGa₂O₄(111) surfaces. In Models S1 and S2, the sulfur atom of the H₂S molecule adsorbed on the Ga_{3c} and Zn_{3c} atoms of the ZnGa₂O₄(111) surface to yield S–Ga and S–Zn bonds with bond lengths of 2.46 Å and 2.50 Å, respectively. In Model S3, the H₂S molecule adsorbed on the O_{3c} atom of the ZnGa₂O₄(111) surface and dissociated to HS[−] and H⁺ ions to form H–O and S–Ga bonds with bond lengths of 0.97 Å and 2.22 Å, respectively. In Model S4, the H₂S molecule moved away from the originally adsorbed O_{4c} atom of the ZnGa₂O₄(111) surface to form an S–Ga bond with a bond length of 2.46 Å. In Models H1 and H2, the H₂S molecules adsorbed on Ga_{3c} and Zn_{3c} atoms of the ZnGa₂O₄(111) surface and dissociated to H⁺ and HS[−] ions to form an H–O bond and an S–Ga bond with bond lengths of 0.97 Å and 2.22 Å, respectively. In Model H3, the hydrogen atom of the H₂S molecule was adsorbed on the O_{3c} atom of the ZnGa₂O₄(111) surface to yield an H–O bond with a bond length of 1.25 Å. In Model H4, the H₂S molecule adsorbed on the O_{4c} atom of the ZnGa₂O₄(111) surface. However, its adsorption was unstable and therefore not ideal, with atomic distances of 3.12 Å and 2.66 Å for H–Ga and H–Zn, respectively.

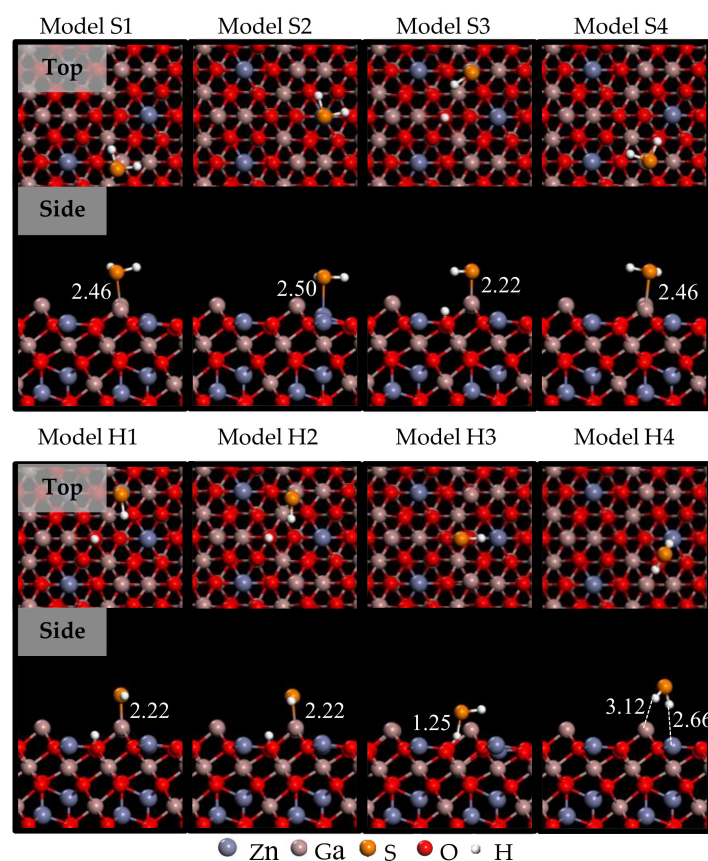


Figure 4. Top and side views of the most favorable configurations for H₂S on the ZnGa₂O₄(111) surface. Atoms are represented by spheres: Zn (purple, large), Ga (brown, large), S (yellow, medium-sized), O (red, medium-sized), and H (white, small). Equilibrium bond lengths between molecular and surface atoms are given in Angstrom.

The vacuum energy, Fermi energy, work functions of ZnGa₂O₄(111) with and without H₂S, and work function difference among H₂S adsorption models are listed in Table 2. The work function difference among Models S1, S2, and S4 decreased when the H₂S molecules adsorbed on the Ga_{3c} and Zn_{3c} atoms of the ZnGa₂O₄(111) surface. The decrease in work function ranged from −0.31 to −1.66 eV, which concurs with the experimental results of other studies showing similar resistance responses of ZnO(Ga) samples to H₂S [11]. Similarly, the H₂S molecule preferred bonding with the Ga_{3c} or Zn_{3c} atom. Model S1 had the maximum work function difference of −1.66 eV, showing increased sensitivity for detecting H₂S molecules. Models S3, H1, H2, H3, and H4 had positive work function differences,

possibly because of the heterolytic break of the H–S bond in the H₂S, resulting in the tendency of forming H–O bonds on the surface of ZnGa₂O₄. The H–S bond-breaking leading to the decrease of the H₂S adsorption might explain the observed change in the decreased sensitivity for detecting H₂S molecules, in agreement with the experimental observation [11].

Table 2. Calculated vacuum energy E_{VAC} , Fermi energy E_F , work function of H₂S Φ_{H_2S} , work function of ZnGa₂O₄(111) Φ_{ZGO} , and work function difference $\Delta\Phi$ ($\Delta\Phi = \Phi_{H_2S} - \Phi_{ZGO}$) among the eight H₂S adsorption models. All energies are presented in eV.

Models	Adsorption Sites	E_{VAC}	E_F	Φ_{H_2S}	Φ_{ZGO}	$\Delta\Phi$
ZnGa ₂ O ₄ (111)	-	0.66	-3.38	-	4.04	-
S1	Ga _{3c}	-0.37	-2.75	2.38	-	-1.66
S2	Zn _{3c}	0.54	-3.19	3.73	-	-0.31
S3	Ga _{3c} , O _{3c}	0.91	-3.32	4.23	-	+0.19
S4	Ga _{3c}	-0.51	-2.91	2.40	-	-1.64
H1	Ga _{3c} , O _{3c}	0.90	-3.32	4.22	-	+0.18
H2	Ga _{3c} , O _{3c}	0.94	-3.32	4.26	-	+0.22
H3	O _{3c}	0.79	-3.37	4.16	-	+0.12
H4	-	0.85	-3.47	4.32	-	+0.28

4. Conclusions

The adsorption reactions and work functions of NO₂ and H₂S on ZnGa₂O₄(111) surfaces were studied using first-principles DFT–GGA calculations. Our results showed that the bonding of the nitrogen (sulfur) atom from a single NO₂ (H₂S) molecule to the Ga atom of Ga–Zn–O-terminated ZnGa₂O₄(111) surfaces exhibited the highest work function change of +0.97 eV (−1.66 eV). Experiments on the resistance responses of ZnO(Ga) samples to NO₂ (H₂S) molecules revealed that sensitivity responses to NO₂ (H₂S) molecules of ZnGa₂O₄-based thin-film sensors exhibit the same trend as that of positive (negative) work function differences [11]. In our favorable configuration, both NO₂ and H₂S molecules preferred bonding with the Ga_{3c} atom of Ga–Zn–O-terminated ZnGa₂O₄(111) surfaces. The results demonstrate the sensitivity responses to NO₂ and H₂S molecules of ZnGa₂O₄-based thin-film sensors, which concur with experimental observations of ZnGa₂O₄-based gas sensors. The thin-film pretreatment technology, such as the thin-film coatings resulting in a Ga-terminated surface, could enhance the sensitivity responses of future gas-sensing devices.

Author Contributions: Conceptualization, J.-C.T. and P.-L.L.; methodology, Y.-H.C. and D.-Y.W.; validation, Y.-H.C. and D.-Y.W.; formal analysis, J.-C.T., Y.-H.C., D.-Y.W., and P.-L.L.; investigation, Y.-H.C. and D.-Y.W.; writing—original draft preparation, J.-C.T. and P.-L.L.; writing—review and editing, J.-C.T. and P.-L.L.; supervision, P.-L.L. All authors have read and agreed to the published version of the manuscript.

Funding: This research was funded by the Ministry of Science and Technology (MOST), Taiwan, grant numbers 109-2221-E-005-042 and 108-2221-E-005-001.

Acknowledgments: Computational studies were performed using the resources of the National Center for High Performance Computing, Taiwan. This manuscript was edited by Wallace Academic Editing.

Conflicts of Interest: The authors declare no conflict of interest.

References

1. Yamazoe, N. Toward Innovations of Gas Sensor Technology. *Sens. Actuators B Chem.* **2005**, *108*, 2–14. [[CrossRef](#)]
2. Meixner, H.; Lampe, U. Metal Oxide Sensors. *Sens. Actuators B Chem.* **1996**, *33*, 198–202. [[CrossRef](#)]
3. Kolmakov, A.; Zhang, Y.; Cheng, G.; Moskovits, M. Detection of CO and O₂ using Tin Oxide Nanowire Sensor. *Adv. Mater.* **2003**, *15*, 997–1000. [[CrossRef](#)]
4. Schwebel, T.; Fleischer, M.; Meixner, H. A Selective Temperature Compensated O₂ Sensor based on Ga₂O₃ Thin Films. *Sens. Actuators B Chem.* **2002**, *65*, 176–180. [[CrossRef](#)]

5. Liu, Z.; Yamazaki, T.; Shen, Y.; Kikuta, T.; Nakatani, N.; Li, Y. O₂ and CO Sensing of Ga₂O₃ Multiple Nanowire Gas Sensors. *Sens. Actuators B Chem.* **2008**, *129*, 666–670. [[CrossRef](#)]
6. Satyanarayana, L.; Reddy, C.V.G.; Manorama, S.V.; Rao, V.J. Liquid-Petroleum-Gas Sensor Based on a Spinel Semiconductor ZnGa₂O₄. *Sens. Actuators B Chem.* **1998**, *46*, 1–7. [[CrossRef](#)]
7. Jiao, Z.; Ye, G.; Chew, F.; Li, M.; Liu, J. The Preparation of ZnGa₂O₄ Nano Crystals by Spray Coprecipitation and its Gas Sensitive Characteristics. *Sensors* **2002**, *2*, 71–78. [[CrossRef](#)]
8. Chen, I.-C.; Lin, S.-S.; Lin, T.-J.; Hsu, C.-L.; Hsueh, T.J.; Shieh, T.-Y. The Assessment for Sensitivity of a NO₂ Gas Sensor with ZnGa₂O₄/ZnO Core-Shell Nanowires—a Novel Approach. *Sensors* **2010**, *10*, 3057–3072. [[CrossRef](#)] [[PubMed](#)]
9. Sung, D.; Hong, S.; Kim, Y.-H.; Park, N.; Kim, S.; Maeng, S.L.; Kim, K.-C. *Ab initio* study of the Effect of Water Adsorption on the Carbon Nanotube Field-Effect Transistor. *Appl. Phys. Lett.* **2005**, *87*, 243110. [[CrossRef](#)]
10. Yuan, Q.; Zhao, Y.-P.; Li, L.; Wang, T. *Ab Initio* Study of ZnO-Based Gas-Sensing Mechanisms: Surface Reconstruction and Charge Transfer. *J. Phys. Chem.* **2009**, *C113*, 6107–6113. [[CrossRef](#)]
11. Vorobyeva, N.; Romyantseva, M.; Filatova, D.; Konstantinova, E.; Grishina, D.; Abakumov, A.; Turner, S.; Gaskov, A. Nanocrystalline ZnO(Ga): Paramagnetic Centers, Surface Acidity and Gas Sensor Properties. *Sens. Actuators B Chem.* **2013**, *182*, 555–564. [[CrossRef](#)]
12. Wu, M.-R.; Li, W.-Z.; Tung, C.-Y.; Huang, C.-Y.; Chiang, Y.-H.; Liu, P.-L.; Horng, R.-H. NO gas sensor based on ZnGa₂O₄ epilayer grown by metalorganic chemical vapor deposition. *Sci. Rep.* **2019**, *9*, 7459. [[CrossRef](#)] [[PubMed](#)]
13. Kresse, G.; Furthmüller, J. Efficiency of *Ab-initio* Total Energy Calculations for Metals and Semiconductors using a Plane-Wave Basis Set. *Comput. Mater. Sci.* **1996**, *6*, 15–50. [[CrossRef](#)]
14. Kresse, G.; Furthmüller, J. Efficient Iterative Schemes for *Ab initio* Total-Energy Calculations using a Plane-Wave basis Set. *Phys. Rev.* **1996**, *B54*, 11169–11186. [[CrossRef](#)] [[PubMed](#)]
15. Kresse, G.; Hafner, J. Norm-Conserving and Ultrasoft Pseudopotentials for First-Row and Transition Elements. *J. Phys. Condens. Matter* **1997**, *6*, 8245–8257. [[CrossRef](#)]
16. Perdew, J.P.; Wang, Y. Accurate and Simple Density Functional for the Electronic Exchange Energy: Generalized Gradient Approximation. *Phys. Rev.* **1986**, *B3*, 8800–8802. [[CrossRef](#)] [[PubMed](#)]
17. Jia, C.; Fan, W.; Yang, F.; Zhao, X.; Sun, H.; Li, P.; Liu, L. A Theoretical Study of Water Adsorption and Decomposition on Low-Index Spinel ZnGa₂O₄ Surfaces: Correlation between Surface Structure and Photocatalytic Properties. *Langmuir* **2013**, *29*, 7025–7037. [[CrossRef](#)] [[PubMed](#)]
18. Kahn, A. Fermi Level Work Function and Vacuum Level. *Mater. Horiz.* **2016**, *3*, 7–10. [[CrossRef](#)]
19. Sahm, T.; Gurlo, A.; Barsan, N.; Weimar, U. Basics of oxygen and SnO₂ Interaction Work Function Change and Conductivity Measurements. *Sens. Actuators B Chem.* **2006**, *118*, 78–83. [[CrossRef](#)]

Publisher’s Note: MDPI stays neutral with regard to jurisdictional claims in published maps and institutional affiliations.



© 2020 by the authors. Licensee MDPI, Basel, Switzerland. This article is an open access article distributed under the terms and conditions of the Creative Commons Attribution (CC BY) license (<http://creativecommons.org/licenses/by/4.0/>).